Progress In Electromagnetics Research C, Vol. 13, 19–32, 2010

EFFECTS OF DC-BIAS CONDITIONS ON LOW-LOSS THIN FILM MICROSTRIP LINE

H.-W. Wu

Department of Computer and Communication
Kun Shan University
No. 949, Dawan Road, Yongkang City, Tainan County 71003, Taiwan

M.-H. Weng

Medical Devices and Opto-electronics Equipment Department
Metal Industries Research & Development Center
1001 Kaonan Highway, Kaohsiung 811, Taiwan

Abstract—This paper presents the microwave characteristics of thin film microstrip line (TFML) under dc-bias conditions. The proposed TFML with 20 μm thick polyimide layer is used as a thin dielectric supporter on low-resistivity silicon (LRS) substrate. Measured frequency-dependent microwave characteristics and equivalent lumped elements are evaluated for the dc-biased TFML over 1–50 GHz. This work presents acceptable attenuation of 0.561, 0.563 and 0.565 dB/mm at 50 GHz with dc-bias conditions, showing that the TFML can be used for high frequency interconnects for any 3D-based microwave devices and monolithic microwave integrated circuits (MMICs).

1. INTRODUCTION

Thin film microstrip lines (TFMLs) are widely used in microwave monolithic integrated circuits (MMICs) as interconnects and matching network circuits. Low-loss and compact transmission lines based interconnects are absolutely critical factor in order to achieve high performance MMICs. In the past, interconnects on the low-resistivity silicon (LRS, $\rho \leqq 10\,\Omega$-cm, ρ is the resistivity of silicon) would generate significant losses, as a result of large coupling between signal line and silicon substrate [1–4].

Recently, some works about TFML-based achievements have been reported [5–7, 9]. Ponchak et al. proposed the characterization of the

Corresponding author: H.-W. Wu (qqq25q@gmail.com).

TFML on thin-film-based polyimide dielectrics [5–7]. The authors presented an in depth characterization of thin film microstrip lines and coplanar waveguide (CPW) lines for MMICs. Leung et al. proposed the silicon-based low-loss coplanar waveguide (CPW) interconnections with low-K dielectric benzocyclobutene (BCB) and self-aligned electroplating of copper [10]. Coplanar waveguide lines with different line widths and line spacings are investigated and compared. Six et al. proposed the characterization and fabrication of silicon-based transmission lines with BCB layer up to 220 GHz [11]. Lee et al. proposed the surface finishing method based on magnetorheological fluid to obtain low-loss high-frequency transmission lines and filters on CMOS-grade silicon [12]. Even though the previous works are capable of overcoming the microwave losses on the low-resistivity silicon substrate, the TFML with dc-bias conditions are not evaluated. From [13–15], we proposed the detailed fabricating process and losses of the TFML without dc-bias conditions. In [15], the equivalent lumped elements of the TFML within 1 volt dc-bias condition are

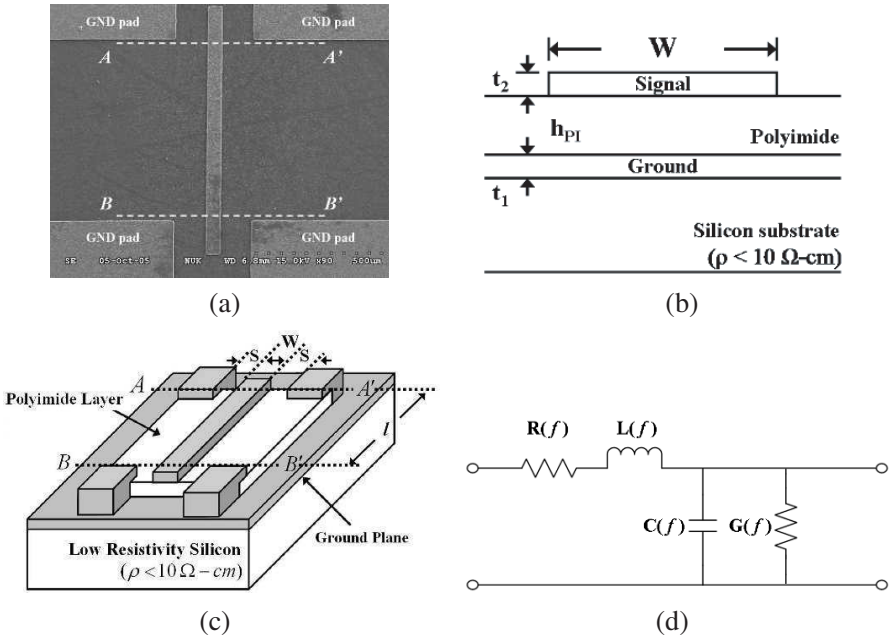

Figure 1. (a) Top view, (b) cross-section configuration, (c) 3-D view and (d) lumped-element equivalent circuit of the thin film microstrip line (TFML). ($W = 60\,\mu m$, $t_1 = 2\,\mu m$, $t_2 = 2\,\mu m$, $h_{PI} = 20\,\mu m$, and length (l) of the TFML is 2000 μm.)

well extracted. The equivalent lumped elements can be effectively contributed to further study on the characteristics of the dc-biased TFML in this work.

In this paper, the effects of the dc-bias conditions on the low-loss TFML are presented. The TFML has been fabricated, as shown in Figure 1. The main goal of this study is to evaluate the measured results before and after applying the dc-bias conditions. The supply voltages on the MMICs will be equal to or less than 1 volt after 2010 [16], and the dc-bias conditions on the interconnects are deserved to be mentioned for evaluating the characteristics of the TFML in MMICs. The measured parameters such as frequency-depend attenuations, effective loss tangent, effective dielectric constant ($\varepsilon_{eff}(f)$), characteristic impedance ($Z_0(f)$) and equivalent lumped elements (RLGC) of the dc-biased TFML have been evaluated. Theoretical studies are performed using 3-D electromagnetic (EM) simulation [17], and the results are confirmed by on-wafer measurement.

2. EXPERIMENTS

Figures 1(a)–(c) show the configuration of the thin film microstrip line (TFML). The TFML is fabricated on 540 µm thick p-type low-resistivity silicon ($\rho \leqq 10\,\Omega$-cm) substrate with $< 1, 0, 0 >$ crystal orientation. Kapton HN-types polyimide (dielectric constant $\varepsilon_r = 3$ at 1 KHz) is used. The starting materials are dianhydride and diamine, all provided by Eternal Ltd. Signal line width (W) is 60 µm, and length 2000 µm) of the TFML is selected. The 2 µm of Al layer as the ground plane of the device is achieved through the dc-sputtering deposition (t_1). The 20 µm of polyimide film (h_{PI}) is obtained using the spin-coating of two successive layers of 10 µm. The average grain size of sputtered Al layer on conductor line and ground plane is 1.2 µm and 0.95 µm observed by scanning electronic microscope (SEM). This technology can effectively develop the high-performance passives and interconnections in MMICs.

3. RESULTS

3.1. Without dc-bias Conditions

Measurements were taken by an HP 8510C vector network analyzer up to 50 GHz. Short-open-load-through (SOLT) calibration was performed, with the de-embedding reference planes (A-A' and B-B') set to the ground-signal-ground (GSG) probe tip, as shown in

Figure 1(c). The temperature of laboratory during the measurements was set at 15–20°C. The dc-bias conditions were simultaneously added with GSG probes at the end of the two ports of the thin film microstrip line (TFML). Losses of the TFML are determined by the main contribution of the strip conductor and supporting dielectric layer (since the polyimide is very thin compared with conventional bulk substrate in this work, radiation loss can be neglected). The $\alpha_t(f)$ is the sum of the conductor loss $\alpha_c(f)$, and dielectric loss $\alpha_d(f)$ is determined by

$$\begin{aligned}\alpha_t(f) &= 8.686 \cdot \left[\frac{1}{l}\mathrm{Re}\left\{\ln\left[\frac{(A+D) \pm \sqrt{(A+D)^2-4}}{2}\right]\right\}\right] \\ &= \alpha_c(f) + \alpha_d(f)(\mathrm{dB/mm}) \end{aligned} \quad (1)$$

where l is the length of the TFML, and A and D are typical elements in the $ABCD$ matrix from the measured complex S-parameters. HFSS simulation is used for analyzing the topology and EM wave propagation of the TFML [17]. Figure 2 shows the attenuation of the typical TFML with different thicknesses of 10, 20, and 30 µm. It is obvious that the loss is not significantly decreasing with thickness from 20 to 30 µm. There is only within the order of 0.1 dB/mm variation of the attenuation at 50 GHz, when the dielectric thickness varies from 20 to 30 µm. Therefore, 20 µm thick of the polyimide will be considered as the optimum parameter for the low-loss TFML.

To compare the measured microwave characteristics of the TFML, the summary of these results is given in Table 1. In [11], the attenuation of the TFML is lower than other research achievements at 50 GHz. We recommend that the TFML is the better method to

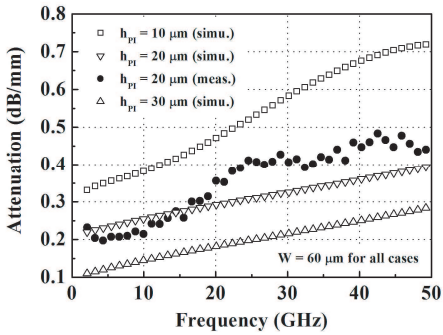

Figure 2. Attenuation of the TFML with different thickness of polyimide film. (Without the dc-bias conditions for all cases.)

Table 1. Comparison of the measured results of the TFML between this work and past literatures. (without dc-bias conditions for all cases) BCB: benzocyclobutene, ML: microstrip line, CPW: coplanar waveguide and X: not shown in the articles.

Ref. year	Line type	Line length/width (μm)	Dielectric layer thickness (μm)	$\varepsilon_{eff}(f)$	$Z_0(f)$ (Ω)	$\alpha_t(f)$ (dB/mm)	$\tan\varepsilon_{eff}(f)$
[8] 1997	ML	X/88	50 (polyimide)	2.8@30 GHz	50	0.18@30 GHz	X
[9] 1998	ML	X/34.4	7.4 (polyimide)	2.6@50 GHz	37	0.38@50 GHz	0.006@avg.
[5] 2001	CPW	X/10	20.15 (polyimide)	1.4@40 GHz	106	0.35@40 GHz	X
[10] 2004	CPW	X/30	20 (BCB)	X	55	0.3@30 GHz	X
[11] 2005	ML	X	20 (BCB)	2.2@50 GHz	50	0.2@50 GHz	0.002@1K Hz
[12] 2007	ML	X/20 X/600	20 (polyimide)	2.38@40 GHz 2.98@40 GHz	88 7	0.32@40 GHz 0.12@40 GHz	X X
Proposed 2010	ML	200/60	20 (polyimide)	1.9@50 GHz	50	0.43@50 GHz	0.004@50 GHz

integrate the passives and active circuits on the silicon substrate due to the advantages of low loss, ease process and good power handling capability in MMICs.

3.2. With dc-bias Conditions

Figure 3(a) shows the configuration of the dc-biased thin film microstrip line (TFML) and related equivalent elements $G(f)$ and $C(f)$ which indicate the conductance and capacitance between the signal line and ground plane. I_g and I_c indicate produced loss current and charged current in polyimide while dc-bias conditions are operated. The dielectric loss in the polyimide with dc-bias conditions is necessary when designing the passives and interconnections in MMICs.

I-V relationship of the dc-biased TFML is shown in Figure 3(b). $I = I_g + I_c$ (where $I_g = G(f)V$, $I_c = j\omega C(f)V$ and V means the applied dc-bias conditions and RF voltage swing). I_g and I_c indicate the in-phase loss current and 90 degree phase difference charged current with applied dc-bias conditions. In order to observe the effects of I_g and I_c of the dc-biased TFML, the frequency-dependent propagation

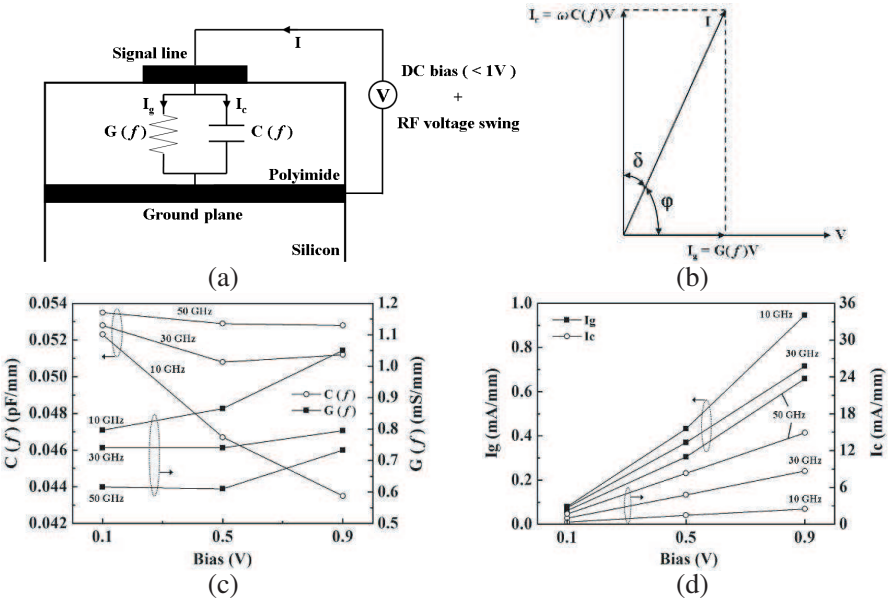

Figure 3. (a) Model, (b) I-V relationship, (c) extracted equivalent lumped element $G(f)$ and $C(f)$ and (d) produced I_g and I_c inside the polyimide when the dc-bias is operated on the thin film microstrip line (TFML). ($G(f)$ means the conductance between the signal line and ground plane, $C(f)$ means the capacitance between the signal line and ground plane, I_g and I_c means the loss current and the charged current produced in polyimide film under dc-bias conditions.)

constant $\gamma(f)$ can be obtained

$$\gamma(f) = \alpha_t(f) + j\beta(f) \tag{2}$$

where $\alpha_t(f)$ is the attenuation constant (from (1)), and $\beta(f)$ is the phase constant. $\gamma(f)$ can be found from the measured complex S-parameters. $\beta(f)$ is determined by

$$\beta(f) = \frac{1}{l}\mathrm{Im}\left\{\ln\left[\frac{(A+D) \pm \sqrt{(A+D)^2 - 4}}{2}\right]\right\} \ (\mathrm{mm}^{-1}) \tag{3}$$

The extracted effective dielectric constant $\varepsilon_{eff}(f)$ and the filling factor q of the TFML can be determined as follows

$$\varepsilon_{eff}(f) = (1-q) + q\varepsilon_r(f) = (\phi_{21} \times c/2\pi f l)^2 \tag{4}$$

where φ_{21} is the phase angle of the TFML from measurement, and f is the frequency. c is the light speed in free space (3×10^8 m/s), and $\varepsilon_r(f)$

is the frequency-depend dielectric constant of the TFML ($f > 1\,\text{GHz}$). q can be calculated as [18]

$$q = 1 - \frac{1}{d}\ln\left(\frac{d+c}{d-c}\right) + \frac{0.732}{d\varepsilon_r(f)}\left[\ln\left(\frac{d+c}{d-c}\right) - \cosh^{-1}(0.358d + 0.595)\right] + \frac{\varepsilon_r(f)-1}{d\varepsilon_r(f)}\left[0.386 - \frac{1}{2(d-1)}\right] \quad (5)$$

where $d = 1 + \sqrt{1+c^2}$ and c is determined from

$$\frac{\pi}{2}\cdot\frac{w}{h_{PI}} = c - \ln\left(c + \sqrt{1+c^2}\right) \quad (6)$$

where h_{PI} and w indicate the thickness of polyimide film and the line width of the TFML. From (4), the frequency-dependent characteristic impedance $Z_0(f)$ of the TFML can be determined as [18]

$$Z_0(f) = \frac{\eta_0}{\sqrt{\varepsilon_r(f)}}\left\{\frac{w}{h_{PI}} + 0.883 + \frac{\varepsilon_r(f)+1}{\pi\varepsilon_r(f)}\left[\ln\left(\frac{w}{2h_{PI}} + 0.94\right) + 1.451\right] + 0.165\cdot\frac{\varepsilon_r(f)-1}{\varepsilon_r^2(f)}\right\}^{-1} \quad (7)$$

for $w/h_{PI} > 2$, where η_0 means the wave impedance for plane waves in free space, and $\varepsilon_r(f)$ can be found from (4). Then the parameters $R(f)$, $L(f)$, $G(f)$, and $C(f)$ were found from [15]. The extracted equivalent elements were summarized in Table 3. Figure 3(c) shows the extracted equivalent lumped elements $G(f)$ and $C(f)$ of the dc-biased TFML. The $G(f)$ is increased with dc-bias increasing from 0.1 to 0.9 volts at the same frequency, indicating that $G(f)$ displays a similar behavior to $R(f)$. Namely, $G(f)$ with higher dc-bias conditions has higher values than that without dc-bias conditions. The $G(f)$ variation is affected by the polarization current in polyimide and uniformity and quality of polyimide. $G(f)$ is also related with dielectric loss of the polyimide, described by the loss tangent. The extracted $C(f)$ of the dc-biased TFML with 0.1 volt, from 1 to 50 GHz, has larger values than those of other dc-biased TFML. These results are caused by the polarization mechanisms of the polyimide under different dc-bias conditions [15]. Figure 3(d) shows the produced charged current I_c inside the polyimide film while dc-bias is operated. The loss current I_g variation is affected by the shunt conductance in polyimide and uniformity and quality of polyimide. When increasing the dc-bias conditions, the I_g in polyimide should be enhanced, and quality of polyimide is reduced, thus the $G(f)$ is increased, as summarized in Table 2.

Figure 4(a) shows the measured frequency-dependent effective dielectric constant $\varepsilon_{eff}(f)$ of the dc-biased TFML. When frequency

Table 2. Extracted equivalent lumped elements of the dc-biased TFML.

dc-bias (V)	Frequency (GHz)	$R(f)$ (Ω/mm)	$L(f)$ (nH/mm)	$G(f)$ (mS/mm)	$C(f)$ (pF/mm)
without dc-bias	10	0.7243	0.1143	0.3292	0.0517
	30	1.2714	0.1121	0.5633	0.0497
	50	1.2503	0.1132	0.5604	0.0504
0.1 V	10	1.3622	0.1231	0.7972	0.0523
	30	1.7007	0.1194	0.7411	0.0528
	50	1.7811	0.1231	0.6162	0.0535
0.5 V	10	2.2133	0.1191	0.8653	0.0467
	30	1.7541	0.1212	0.7413	0.0508
	50	1.3822	0.1211	0.6111	0.0529
0.9 V	10	2.8731	0.1198	1.0512	0.0435
	30	1.8633	0.1204	0.7954	0.0512
	50	1.6723	0.1221	0.7331	0.0528

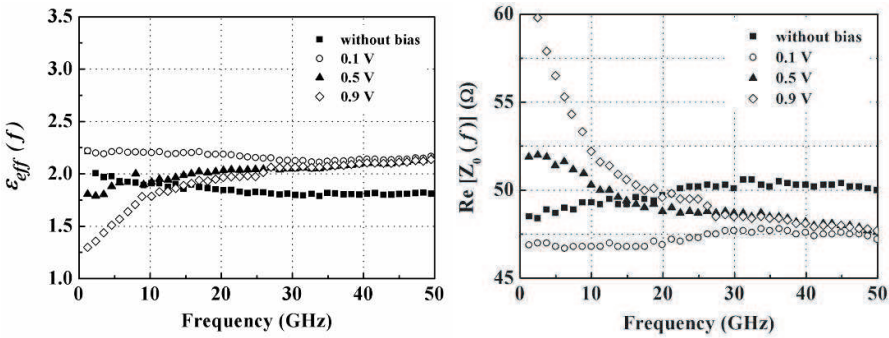

Figure 4. Measured frequency-dependent (a) effective dielectric constant $\varepsilon_{eff}(f)$ and (b) real part of the characteristic impedance $\mathrm{Re}[Z_0(f)]$ of the dc-biased TFML.

increases over 1 to 50 GHz, the extracted $\varepsilon_{eff}(f)$ shows average value of 1.96, 2.17, 2 and 1.95 with 0, 0.1, 0.5 and 0.9 volts. As without dc-bias conditions, the TFML has a strong slow wave effect which is due to the high conductor loss resulting from the small ratio of metal line thickness of skin depth at lower frequencies. In [19], the extracting method is used by 3-D electromagnetic simulation to

confirm the effects of the line widths on the $\varepsilon_{eff}(f)$ variations within $\pm 5\%$ over 1–50 GHz. Figure 4(b) shows the measured frequency-dependent real part of $Z_0(f)$ of the dc-biased TFML. The extracted $\mathrm{Re}[Z_0(f)]$ of the TFML without dc-bias is maintained in the range of $47.5\Omega < Z_0(f) < 50.2\Omega$ over 1–50 GHz, which are suitable for integrating the passives and active devices on the low-resistivity silicon substrate. With increasing the dc-bias conditions, the $\mathrm{Re}[Z_0(f)]$ is progressively increased below 30 GHz, except that with 0.1 volt, and becomes nearly constant ($47.8\Omega < Z_0(f) < 48.3\Omega$) above 30 GHz.

Figure 5 shows the measured frequency-dependent attenuation $\alpha_t(f)$ of the dc-biased TFML. With increasing the dc-bias conditions, the attenuation is also increasing below 30 GHz and achieves a similar value between 0.4 and 0.6 dB/mm. Conductor loss $\alpha_c(f)$ of the dc-biased TFML can be calculated from $Z_0(f)$. The series distributed resistance in ohms per unit length of the conductor R_1 and the series distributed resistance in ohms per unit length of the ground plane R_2 must be evaluated as follows [20]

$$\alpha_c(f) = 8.686 \times \frac{R_1 + R_2}{2Z_0(f)} \ (\mathrm{dB/mm}) \tag{8}$$

R_1 and R_2 are determined as

$$R_1 = \frac{R_s}{w} LR \left(\frac{1}{\pi} + \frac{1}{\pi^2} \ln \frac{4\pi w}{t_2} \right) \ (\Omega/\mathrm{mm}) \tag{9}$$

where LR is the loss ratio which gives the increase in resistance that results from an unequal division of the current [20], and t_2 is the thickness of conductor. Skin resistance $R_s = 1/\delta\sigma$ (δ is the skin depth, and σ is the conductivity of conductor material.)

$$R_2 = \frac{R_s}{w} \left(\frac{w/h_{PI}}{w/h_{PI} + 5.8 + 0.03 h_{PI}/w} \right) \ (\Omega/\mathrm{mm}), \ 0.1 < \frac{w}{h_{PI}} \leq 10 \tag{10}$$

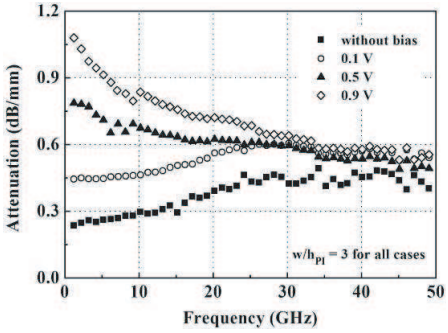

Figure 5. Measured attenuation of the dc-biased TFML.

Conductor loss influenced by skin effect at different metal thicknesses and geometry dependence is considered in R_1, and conductor loss influenced by the ground plane and geometry dependence is considered in R_2.

Figure 6(a) shows the measured frequency-dependent conductor loss of the dc-biased TFML. It is clear that $\alpha_c(f)$ is almost dependent on frequency due to the change of current-density distribution in the nonideal conductors. With increasing the dc-bias conditions, the $\alpha_c(f)$ is increased around an average of 1.3% over 1–50 GHz. It is seen that the measured $\alpha_c(f)$ is more related to the filling factor q of the TFML.

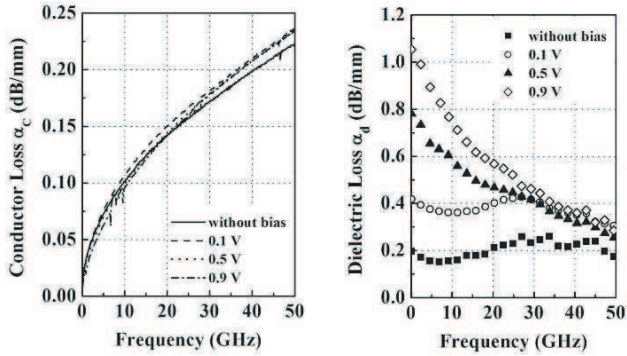

(a) (b)

Figure 6. Measured frequency-depend (a) conductor loss and (b) dielectric loss of the dc-biased TFML.

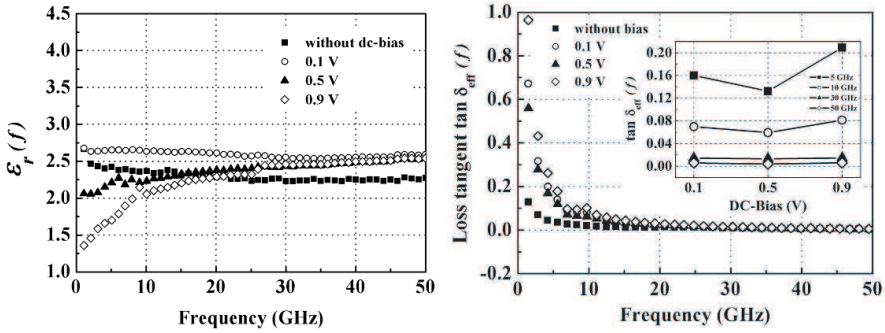

(a) (b)

Figure 7. Measured frequency-depend (a) dielectric constant $\varepsilon_r(f)$ and (b) effective loss tangent $\tan\delta_{eff}(f)$ of the dc-biased TFML.

Dielectric loss $\alpha_d(f)$ of the dc-biased TFML can be calculated by

$$\alpha_d(f) = \alpha_t(f) - \alpha_c(f) \text{ (dB/mm)} \tag{11}$$

$\alpha_d(f)$ variations with increasing the dc-bias conditions caused by the loss current (polarization current, I_g) in dielectric layer and uniformity and quality of polyimide are dominated, as shown in Figure 6(b). The $\alpha_d(f)$ is proportional to the voltage across the polyimide material. Therefore, standing waves of voltage on a line increase the order of $\alpha_d(f)$ [21]. Under an applied electric field, the dielectric material stores energy in the form of an electric charge. Many of these charge carriers are naturally polarized dipoles and realign themselves by rotation in the direction of the applied electric field, especially in the frequency range from 1 MHz to 10 GHz [21]. As the result of this rotation, part of the electrical energy is converted into heat and is lost.

Figure 7(a) shows the measured frequency-dependent dielectric constant $\varepsilon_r(f)$ of the dc-biased TFML. The average dielectric constant $\varepsilon_r(f)$ is found to be 2.3 without bias, 2.6 with 0.1 V, 2.4 with 0.5 V, and 2.3 with 0.9 V over 1–50 GHz. Dispersion effects can be neglected to microstrip line on the proposed polyimide, indicating an excellent dielectric stable material and suitable for high frequency substrate. The average frequency-dependent effective loss tangent $\tan\delta_{eff}(f)$ of the TFML with dc-bias conditions can be calculated by

$$\tan\delta_{eff}(f) = \frac{\alpha_d(f)\sqrt{\varepsilon_{eff}(f)}\,(\varepsilon_r(f)-1)\,\lambda_0}{27.3\varepsilon_r(f)\,(\varepsilon_{eff}(f)-1)} \tag{12}$$

Table 3. Measured microwave characteristics of the dc-biased TFML.

dc-bias (V)	Frequency (GHz)	$\varepsilon_{eff}(f)$	$Z_0(f)$ (Ω)	$\alpha_t(f)$ (dB/mm)	$\alpha_c(f)$ (dB/mm)	$\alpha_d(f)$ (dB/mm)	$\tan\varepsilon_{eff}(f)$
without dc-bias	10	1.99	49.2	0.255	0.102	0.153	0.015
	30	1.89	50.4	0.444	0.172	0.273	0.009
	50	1.93	50.0	0.438	0.223	0.214	0.004
0.1V	10	2.19	46.9	0.466	0.107	0.358	0.034
	30	2.13	47.5	0.596	0.182	0.414	0.013
	50	2.16	47.3	0.561	0.236	0.325	0.006
0.5 V	10	1.91	50.4	0.677	0.099	0.578	0.062
	30	2.06	48.6	0.589	0.178	0.411	0.014
	50	2.14	47.7	0.563	0.234	0.229	0.004
0.9 V	10	1.78	52.3	0.843	0.096	0.747	0.082
	30	2.07	48.4	0.634	0.179	0.455	0.015
	50	2.13	47.7	0.565	0.234	0.328	0.006

where λ_0 indicates the wavelength in free space. The average effective loss tangent $\tan\delta_{eff}(f)$ is found to be 0.008 without bias, 0.014 with 0.1 V, 0.026 with 0.5 V, and 0.034 with 0.9 V over 1–50 GHz, as shown in Figure 7(b) and summarized in Table 3.

4. CONCLUSION

In this paper, we have fabricated and characterized the TFML with dc-bias conditions within 1 volt. The microwave characteristics of the dc-biased TFML have been compared with previous works, as summarized in Table 3. Through the standard CMOS fabrication process and on-wafer measurement, this study can provide a new evaluation for determining the microwave characteristics of the dc-biased TFML for high dense and high-performance interconnects in MMICs. Finally, the TFML-based interconnects can be further applied to automotive radar applications at above 77 GHz in multi-chip-module-deposition (MCM-D) and monolithic microwave integrated circuits (MMICs).

ACKNOWLEDGMENT

The authors wish to acknowledge Mr. Y. D. Lin for sample preparation and the funding support from Nation Science Council of Taiwan, under Grant NSC 98-2218-E-168-003.

REFERENCES

1. Tummala, R. R. and E. J. Rayaszewski, *Microelectronic Packaging Handbook*, Van Nostrand Reinold, New York, 1989.
2. Baliga, J., "System-in-package uses silicon substrate," *Semicond. Int.*, Vol. 27, 32, 2004.
3. Luy, J. F. and P. Russer, *Silicon-based Millimeter-wave Devices, Ser. Springer Series in Electronics and Photonics*, Springer-Verlag, Berlin, Germany, 1994.
4. Chang, J. Y. C., A. A. Abidi, and M. Gaitan, "Large suspended inductors on silicon and their use in a 2-μm CMOS RF amplifier," *IEEE Electron Device Lett.*, Vol. 14, 246–248, 1993.
5. Ponchak, G. E., A. Margomenos, and L. P. B. Katehi, "Low-loss CPW on low-resistivity Si substrates with a micromachined polyimide interface layer for RFIC interconnects," *IEEE Trans. Microwave Theory Tech.*, Vol. 49, 866–870, 2001.
6. Ponchak, G. E. and L. P. B. Katehi, "Measured attenuation of coplanar waveguide on CMOS grade silicon substrate with

polyimide interface layer," *IEE Electron. Lett.*, Vol. 34, 1327–1329, 1998.

7. Ponchak, G. E., "RF transmission lines on silicon substrate," *Proc. 29th Eur. Microwave Conf.*, 158–161, Oct. 1999.
8. Nakatsugawa, M., A. Kanda, H. Okazaki, K. Nishikawa, and M. Muraguchi, "Line-loss and size reduction techniques for millimeter-wave RF front-end boards by using a polyimide/alumina–ceramic multilayer configuration," *IEEE Trans. Microwave Theory Tech.*, Vol. 45, 2308–2315, 1997.
9. Ponchak, G. E. and A. N. Downey, "Characterization of thin film microstrip lines on polyimide," *IEEE Trans. Comp. Pack. Manufact. Technol.,* Vol. 21, 171–176, 1998.
10. Leung, L. L. W., W. C. Hon, and K. J. Chen, "Low-loss coplanar waveguides interconnects on low-resistivity silicon substrate," *IEEE Trans. Comp., Packag., Manufact. Technol.*, Vol. 27, 507–512, 2004.
11. Six, G., G. Prigent, G. Dambrine, and H. Happy, "Fabrication and characterization of low-loss TFMS on silicon substrate up to 220 GHz," *IEEE Trans. Microwave Theory Tech.*, Vol. 53, 301–305, 2005.
12. Lee, S. N., J. I. Lee, Y. J. Kim, and J. G. Yook, "Low-loss thin film microstrip lines and filters based on magnetorheological finishing," *IEEE Trans. Comp. Packag. Technol.,* Vol. 30, 849–854, 2007.
13. Wu, H. W., M. H. Weng, Y. K. Su, and R. Y. Yang, "Characteristics of low k thin film microstrip line on standard lossy silicon substrate for radio frequency integrated circuits," *Microw. Opt. Techn. Lett.*, Vol. 49, 79–83, 2007.
14. Wu, H. W., Y. K. Su, R. Y. Yang, M. H. Weng, and Y. D. Lin, "Fabrication of low loss thin film microstrip line on low resistivity silicon for RF applications," *Microelectronics J.*, Vol. 38, 304–309, 2007.
15. Wu, H. W., M. H. Weng, Y. K. Su, R. Y. Yang, and C. Y. Hung, "Equivalent lumped elements of dc-biased thin film microstrip line in MMICs," *IEEE Microwave and Wireless Components Letters*, Vol. 17, 673–675, 2007.
16. "International technology roadmap for semiconductors (ITRS), radio frequency and analog/mixed-signal technologies for wireless communications," Ch. 9, 2007 update.
17. HFSS, Ansoft, Palo Alto, CA.
18. Gupta, K. C., R. Garg, I. Bahl, and P. Bhartia, *Microstrip Lines and Slotlines*, 2nd edition, Artech House, 1996.

19. Janezic, M. D., D. F. Williams, V. Blaschke, A. Karamchrti, and C. S. Chang, "Permittivity characterization of Low-k thin film from transmission-line measurements," *IEEE Trans. Microwave Theory Tech.*, Vol. 51, 132–136, 2003.
20. Collin, R. E., *Foundations for Microwave Engineering*, McGraw-Hill, Inc., 1992.
21. Tummala, R. R., *Fundamentals of Microsystems Packaging*, McGraw-Hill, Inc., 2001.